Crack Tip Flipping under Mode I Tearing: Investigated by X-Ray Tomography

Nielsen, Kim Lau; Gundlach, Carsten

Published in:
International Journal of Solids and Structures

Link to article, DOI:
10.1016/j.ijsolstr.2017.04.014

Publication date:
2017

Document Version
Peer reviewed version

Crack Tip Flipping under Mode I Tearing: Investigated by X-Ray Tomography

Kim Lau Nielsen[1*] and Carsten Gundlach[2]

[1)] Department of Mechanical Engineering, Solid Mechanics, Technical University of Denmark, DK-2800 Kgs. Lyngby, Denmark

[2)] Department of Physics, Imaging, Technical University of Denmark, DK-2800 Kgs. Lyngby, Denmark

---

Abstract – The fracture surface morphology that results from mode I tearing of ductile plate metals depends heavily on both the elastic-plastic material properties and the microstructure. Severe tunneling of the advancing crack tip (resulting in cup-cup, or bath-tub like fracture surfaces) can take place in a range of materials, often of low strength, while tearing of high strength metals typically progress by the shear band failure mechanism (slanting). In reality, however, most fracture surfaces display a mixture of morphologies. For example, slant crack propagation can be accompanied by large shear lips near the outer free plate surface or a complete shear band switch - seemingly distributed randomly on the fracture surface. The occasionally observed shear band switch of mode I slant cracks, related to ductile plate tearing, is far from random as the crack can flip systematically from one side to the other in roughly 45-degree shear bands. This "flipping" action of a slanted crack remains to be fully understood, and the present study serves to share details on the phenomenon by exploiting X-ray tomography scanning to access the plate interior and the very crack tip. Throughout, the focus is on a crack tip where the flip is underway. Extensive growth of single edge cracks under mode I loading is achieved in a purpose build test set-up. Here, considering a 4 mm plate of normal strength / high strain hardening steel which has been found to display successive flipping of the slant crack face. While undergoing a shear band switch, such that the flipping mechanism is active, the plate tearing test is interrupted and the crack tip extracted for further investigation. The conducted X-ray tomography scans reveal the failure process ahead of the advancing crack tip to resemble the ductile slant crack growth governed by local thinning and moderate crack tip tunneling. However, small shear lips form at the outer free plate surface, well behind the 45-degree slant (tunneling) crack tip, as the flipping action engages. Upon further loading, the shear lips subsequently grow to form a set of secondary crack fronts at an angle to the primary tunneling slant crack. Eventually, these secondary crack fronts catch up on the primary slant crack front and overtake the growth to complete the shear band switch. Once the crack slants, an

out-of-plane action occurs due to the loss of symmetry in the system. It is this out-of-plane action which is believed to set-off the flipping mechanism.

Keywords: Plate tearing, Shear band switch, Crack tip shape, Ductile failure

---

* Corresponding author

Tel: (+45) 4525-4258, Fax: (+45) 4593-1475

Email address: kin@mek.dtu.dk (K.L. Nielsen)

1. Introduction

The micro-mechanisms governing ductile plate tearing have been established through decades of research (Tvergaard, 1990; Benzerga and Leblond, 2010, Pineau et al., 2016). It is well known that ductile failure generally is governed by the process of void nucleation and growth to coalescence at the micron-level (Needleman, 1972; Gurson, 1977, Tvergaard, 1981, 1982a, 1982b; Fleck and Hutchinson, 1986; Koplik and Needleman, 1988; Thomason, 1990; Benzerga, 2002; Liu et al., 2003; Scheyvaerts et al, 2006; Barsoum and Faleskog, 2007a,b; Tvergaard, 2008, 2009; Leblond and Motlet, 2008; Nielsen and Tvergaard, 2011). Intermetallic inclusions are typically responsible for the nucleation of microvoids which grow to coalesce and eventually form microcracks. In the end, it is the formation of such microcracks (or the lack thereof) and their linkages ahead of the advancing crack tip that determines the crack tip shape and propagation mode. For example, different tearing modes, leading to different crack surface morphologies (such as cup-cup, cup-cone, or slanting), have been observed for extensive crack growth in plate metals and the underlying micro-mechanisms are often considered known. This despite of Morgeneyer et al. (2014) recently demonstrating new insight to the localization process at the very tip of a mode I tearing crack in a thin aluminum alloy (2198) sheets by focusing high-resolution in-situ synchrotron X-ray laminography on the phenomenon. Their study indicates that plastic flow localization can precede significant damage evolution and that a burst of nucleating damage sets in at a later stage for Al 2198. Slant crack propagation within 45-degree angled shear bands often occurs in high strength material, whereas a cup-cup (bath-tube like) failure is typically found in low strength / high strain hardening alloys (Pardoen et al., 2004). Despite such insight, the interplay between tearing modes remains to be fully understood and nowhere is a conclusive answer to; *what makes the crack choose one tearing mode over the other,* found. In fact, the reality is that a mixture of the propagation modes typically develops on the fracture surface of same plate such that transitional crack surface morphology appears.

In addition to the established tearing modes (cup-cup, cup-cone, and slanting), strong evidence exists that a portion of the observed transitional crack surface morphology belongs to an overlooked tearing phenomenon nicknamed "crack tip flipping" in El-Naaman and Nielsen (2013). The phenomenon is strongly tied to slant crack propagation, where two equally active shear bands travel, within a heavily strained region in front of the leading crack tip, such that plastic flow and failure eventually localize in one shear band - leaving the other band inactive. The crack thereby propagates in a 45-degree tilted manner (know as crack slanting, see also Mathur et al., 1996; Besson et al., 2003; Nielsen and Hutchinson, 2012, for numerical results). From time to time, however, the propagating crack can switch to the former inactive shear band whereby it flips the 45-degree tilted orientation to the opposite side. Gruben et al. (2013) observed such occasional switches under mode I tearing of dual-phase steel, whereas Rivalin et al. (2001); Simonsen and Törnqvist (2004), Zheng et al. (2009); El-Naaman and Nielsen (2013) have observed successive flipping of the slanted crack in a very systematic manner. Rivalin et al. (2001) conducted a number of tearing experiments on pipeline steel, including both high-speed dynamic tests and quasi-static tests. Clearly, their specimens exhibited the flipping mechanism when subject to high crack growth rates (Fig. 7b in their paper). Zheng et al. (2009) carried out an extensive quasi-static analysis of large welded panels (of 3 mm wall thickness, AA6061 Aluminum) and observed a slant fracture surface alternating at angles ± 45 degree approximately every 60 mm, but within the heat affected zone of the welded joint. Simonsen and Törnqvist (2004), and later El-Naaman and Nielsen (2013), studied extensive crack propagation in plate metal (steel and aluminum) and found cracks propagating by the flipping mechanism in a stable and controlled manner (easily traced by the naked eye), with the crack extending many plate thicknesses. What causes the crack to flip remains to be fully understood, but it is obvious that once localization into one of the two shear bands takes place, the symmetry of the mode I tearing experiment is lost, and a slight out-of-plane deflection of the plate occurs. It is this mode III type loading of the crack that is believed to fertilize the flipping mechanism (see also Felter and Nielsen, 2017; Nielsen and Hutchinson, 2017).

El-Naaman and Nielsen (2013) extracted an isolated flip on the fracture surface of a completed tearing test and polished a number of cross-sections perpendicular to the growth direction to shed light on the steps involved in the flipping process. From this first study, it became evident that the flipping occurs in a symmetric manner as the fracture surface poses 180-degree rotational symmetry about the crack growth direction. Moreover, their study revealed the flipping to rely on the formation of shear lips near the outer free plate surface.

Once formed, these shear lips grow upon loading and eventually merge to form an active shear band to the opposite side (thereby completing the flip). This initial study, however, was conducted on an already completed flip and, hence, do not reveal any details on the crack advance mechanism. For example, one question that arises is; *how do the shear lips interact with the primary slant crack face?*

The present study focuses on the initiation of the flipping action and aims to share details on the evolution of the shear lips, by relying on X-ray tomography scanning to achieve a look into the processes at play as the shear lips initiate and grow to overtake the leading crack tip. To do so, a slanted crack where a flip is underway, rather than an already completed flip, is considered by interrupting a plate tearing experiment just as the flip becomes visible on the outer free plate surface. The study, here, takes as off-set the plate tearing set-up developed in El-Naaman and Nielsen (2013). While interrupted, the test is stopped, and the plate unloaded, to extract samples of the crack tip for further X-ray tomography scanning. Compared to the process of cutting and polishing cross-sections successively along the growth direction (as in El-Naaman and Nielsen, 2013), a much refined sequence of cross-sections are created by used of X-ray tomography, and moreover; the cross-sections are available in multiple views (see for example Figs. 2-6). Thus, the combination of focus on a flip underway and the use of X-ray tomography allow unseen details of the flipping process to be brought out and individual features at the plate interior to be accurately traced. For example, it becomes clear that the primary slant crack face propagates by moderate crack tip tunneling, and that the very tip shows no sign of flipping at a state where the phenomenon becomes obvious to an observer watching the propagating crack on the outer free plate surface. It is, instead, the shear lips that govern the flip as they form well behind the leading tip, then grow and overtakes the primary slant crack face - thus altering the apparent orientation of the slanting crack.

The paper is structured as follows. The experimental procedure including details on the plate tearing experiments, the X-ray tomography scanning, and data analysis are outlined in Section 2. Results and the discussions hereof are presented in Section 3, while Section 4 gives the concluding remarks.

2. Experimental Investigation

2.1 Mode I Tearing Experiments and Sample Preparation

Mechanical testing of mode I tearing in 4 mm normal strength non-alloy structural steel (EN 10025, see Table 1) plates is undertaken to form the basis for a close inspection of the crack tip

when undergoing a shear-band switch (referred as the flipping mechanism). The experiments take as off-set the test set-up discussed in El-Naaman and Nielsen (2013) (initially developed by Simonsen and Törnqvist, 2004), where the crack is allowed to grow roughly 30 plate thicknesses without reaching the far boundaries. Thus, no pre-cracking of the plate was conducted since the crack initiation has no effect on the subsequent flipping mechanism once the crack has propagated several plate thicknesses. Care was taken that extensive crack propagation was achieved for all samples investigated by X-ray Tomography. Details on the material can be found in Table 1 (fitted by El-Naaman and Nielsen, 2013), and a further examination regarding fractographs of the final fracture surface can be found by El-Naaman and Nielsen (2013). Selected areas on the fracture surface all bear the signs of void growth to coalescence. In fact, the fracture surface shows no sign of severely smeared dimples (/voids) as a result of intense shearing.

The test set-up and plate specimen (in gray) are illustrated in Fig. 1a. Here, the plate is loaded in combined tension and in-plane bending (with mode II contributions from the weight of the rig balanced out). All mechanical tests are carried out using a standard MTS Flextest hydraulic machine equipped with a 100 kN load cell. The force, the piston displacement (measured by an MTS LVDT), and the time is recorded during testing. In addition, to measure the crack advance, a grid was applied to the un-deformed specimens along the expected crack path, where after timed still photographs were taken, against a contrasting background, continuously throughout each test. The crack length for a specific force or displacement is extracted by relating the data. A representative set of test results is displayed in Figs. 1b-c (see also El-Naaman and Nielsen, 2013, for more details on the mechanical tests).

In the investigation of the crack tip flipping mechanism, it is important to realize that the flip takes place in a very stable manner and, hence, can easily be traced on the free plate surface by the naked eye. Thus, the tearing test was stopped once crack tip flipping is evident to the operator, and the plate is unloaded, to extract samples of the crack tip for further investigation by X-ray tomography scanning.

2.2 X-ray Tomography and Measuring Procedure

The X-ray tomography scanning experiment was performed using a commercial Zeiss Xradia 410 versa system equipped with a reflection tungsten target X-ray source with a pre-voltage range from 40 kV to 150 kV and a maximum power of 10 watt. Throughout, a high voltage of 150 kV is employed to ensure that the X-ray penetrates the long side of the sample

(approximate 12mm of steel). The sample was mounted using a grip in one end, away from the measuring area, such that undisturbed 360-degree access to the sample was obtained. Each tomography scan is acquired with at least 3201 projections covering the 360-degree rotation of the sample. The reconstruction of scan data relies on a Feldkamp, Davis and Kress algorithm (Feldkamp et al., 1984), based on filtered back-projection algorithm. To bring out the details of the flipping mechanism, the present work employs three different settings for the tomography measurements, these are; i) a large field view measurement with a voxel size of 20.4μm (using 3201 projections), ii) an intermediate field view measurement with voxel size of 4.0μm (using 6401 projections), and iii) a high resolution measurement with voxel size of 1.2μm (using 4001 projections).

2.3 Data Analysis

To visualize the crack tip features in focus, the data generated from the X-ray tomography scanning are approached in three different ways; i) images were extracted as cross-sectional views (Figs. 3-6) using the Software Package "XRControler" developed by Zeiss as part of the X-ray tomography system. This allows easy comparison of different planar cross-sections, as well as a comparison to images from conventional Scanning Electron Microscopy published in the literature. ii) to give a three-dimensional view of the flipping crack tip, image analysis of the raw scanning data was carried out using the MATLAB Software package (see Figs. 7-10a). In these images, additional 2D median filtering (8-by-8 neighbors) of cross-sections in the x_2x_3-plane (see Fig. 2) is added, where after a black-and-white image is generated by identifying the edges using a Sobel method (threshold 0.7)[1]. This post-processing of data was found to bring out the morphology of the fracture surfaces more clearly without compromising the data. iii) to help the interpretation of results a much less detailed approach was taken by manually recording the location of the most essential features (being the primary crack surface and shear lips) in the individual cross-sections (in the x_2x_3-plane). By connecting these essential features with straight lines, and collecting a number of cross-sections, the 3D reconstructions displayed in Figs. 8b-10b were created.

[1] The n-by-m neighbors and the threshold were gradually increased to ensure as little loss of details as possible.

3. Results and Discussion

Results are presented in the following for a number of X-ray tomography scans completed on one particular crack tip where a flip is underway. In light of this, it is worth to mention that the X-ray scans presented in this study are not time resolved, and thus the interpretation of results are strongly tied up on the time history of the crack flipping seen on the outer free plate surface – which is easy to trace and indeed time resolved. Moreover, the early study by El-Naaman and Nielsen (2013) serves as a "temporal resolution" as it reveals the fracture surface morphology for the completed flip. In the present study, the mechanical test of the plate has been interrupted at the very beginning of the flip, and the extracted sample holds thereby the key to the initial configuration of the flipping crack tip. Results are presented for the three different tomography scanning settings with voxel size; 20.4μm (in Fig. 4), 4.0μm (in Figs. 3, 5, and 8-10), and 1.2μm (in Figs. 6-7), corresponding to increased level of details as the resolution is approximately 100μm, 20μm, and 6μm, respectively.

Figure 2 displays the large view scan in full 3D with the cross-sectional planes of main interest defined. Here, displaying the zero-planes with origo at the very crack tip. Throughout the study, the coordinate axes remain fixed such that; the crack propagates along the positive x_1-axis, the x_2-axis is the through-thickness direction, and the plate is loaded along the x_3-axis. Moreover, as tomography scanning essentially reveals changes in density, black/dark regions indicates "air" and bright colors indicate dense material in Figs. 3-6.

A series of cross-sections from the investigated crack tip is shown in Fig. 3. Here considering the x_2x_3-plane to mimic conventional cross-sectional views of cracked metal plates reported in the literature from either optical- or electro-microscopy. The crack propagates away from the reader (along the x_1-axis), such that Figs. 3a and 3f are cross-sections near the crack tip and far behind the crack tip, respectively. Compared to physically cutting and polishing samples a much refined sequence of cross-sections is created by employing X-ray tomography - essentially one cross-sectional image is obtained for every 4.0μm (at intermediate resolution). Thus, the evolution of the individual features is easy to trace in the crack growth direction when going through the full set of scanning images, and only a very small sub-set of the cross-sectional scans is presented here. From Fig. 3 it is, first and foremost, noticed that all cross-sections in the x_2x_3-plane pose 180 degree rotational symmetry about the growth direction. Thus, not only does that surface morphology of the completed flip display this characteristic (as discussed by El-Naaman and Nielsen, 2013), but the present tomography scans reveal that the fracture process itself shows the same behavior.

Figure 3a shows severe thinning of the plate material as well as a small slant crack initiated at mid-thickness; this being the very tip of the primary slant crack face. Through Figs. 3b-c, the width of this slanted primary crack face increases, but remains confined to the interior of the plate such that crack tip tunneling takes place. As a key feature of the flipping mechanism, the crack face makes a roughly 90-degree kink on each side, closer to the free surface (see Fig. 3d), and two small additional protrusions evolve through Figs. 3e-g. By linking these X-ray scans to the history of the flipping crack observed on the outer free plate surface, the protrusions are the evolving shear lips, and their early appearance at the interior of the plate (see Figs. 3d-e) indicates, as well, tunneling of these secondary cracks faces. Thus, it is worth to notice that the slanting crack, when undergoing a flip, consists of two types of leading edges; i) one being the leading edge of the primary slant crack, and ii) one being the leading edge of the evolving shear lips (referred to as secondary crack faces), which connect to the outer free plate surface. Moreover, it is important to realize that the shear lips are not only trailing behind the tip of the primary slanted crack face, but these will eventually catch up and form a slanted crack face to the opposite side - thereby completing the flip. Thus, the leading edge of the shear lips must be traveling at a greater speed than the leading edge of the primary slanted crack face. In fact, there is no evidence of the primary slant crack stops propagating when the shear lips start growing – rather is the opposite the case. By comparing the current tip shape of the primary slant crack to the feature on the fracture surface for the completed flip in El-Naaman and Nielsen (2013), the tunneling of the primary crack tip for the completed flip extends much further before the shear lips covers the entire surface.

Through Figs. 3e-g, the width of the primary crack face continuously increases despite the overall crack face now being kinked such that the slanted primary crack face exists well behind the leading crack tip (see Figs. 3h-f). This clearly demonstrates that the investigated sample indeed holds the very initiation of the flipping mechanism.

The severe thinning of this particular steel becomes very obvious when considering the cross-sections of the large field view scan in Fig. 4 (100μm resolution). Here, considering planar cross-sections in the x_1x_2-plane at three different levels along the loading direction (x_3-axis). The dashed lines define the outer contour in the individual cross-sections. Figures 4a and 4c display cross-sections above and below the zero-plane, respectively, with the zero-plane taken to be the plane where the leading crack tip has advanced the furthest (see also Fig. 2 where black indicates "air" and bright colors indicate dense material). From Fig. 4b it is seen that the zero-plane only bears sign of one evolving crack face (the primary slant crack face).

This has to do with the flip being in an early state such that the shear lips near the outer free plate surface (observed in Fig. 3) have not yet intersected the zero-plane. However, by lowering (or lifting) the plane for this cross-sectional view along the x_3-axis, the primary crack face is found to connect to the shear lips (secondary crack faces) located on the left hand (or right hand) side. To add details to this co-existence of the secondary and the primary crack faces, additional scans at intermediate (20μm) and high (6μm) resolution are performed. Similar to Fig. 4, these results are depicted in Figs. 5 and 6 as cross-sectional views in the x_1x_2-plane. Figure 5 displays cross-sections at five different levels along the loading direction (x_3-direction), with Fig. 5a being the top plane, Fig. 5c the zero-plane, and Fig. 5d the bottom plane. As for the low resolution scan, Fig. 5c indicates that only the primary crack face exists at the zero-plane, whereas; by moving the cross-sectional view along the x_3-axis towards the top (or bottom) it becomes clear that the primary crack face connects to the secondary crack face near the outer free plate surface (dashed lines). In particularly, this is evident from Figs. 5a and 5e (also notice that Figs. 5a and 5e are essential each other mirror). The connection of the primary and secondary crack faces is, however, somewhat doubtful in Figs. 5b and 5d, and the question is *if the connection between the two cracks faces is really there?* To shed light on this, a high resolution scan (6μm) was performed for one of the shear lips (see Fig. 6). From these results it is clear, that the secondary and primary crack face connects near the outer free plate surface (Figs. 6a-b), but also that the connection is interrupted when moving closer to the zero-plane (Figs. 6c-d). In fact, Fig. 6d clearly displays two separate crack faces. This has to do with the three dimensional nature of the flipping crack tip. The shear lips (being the secondary crack faces) are largest near the outer free plate surface and, thus, intersect with cross-sectional x_1x_2-planes closer to the zero-plane.

To bring out the three-dimensional nature of the flipping crack, the raw data from the X-ray tomography scanning have been exploited to obtain both automatically and manually reconstructed 3D images. Figure 7 depicts an automatically generated (using image analysis and filtering, see Section 2.3) reconstruction of the shear lip based on the high-resolution scan (6μm). Here, showing a part of the primary slanted crack face and the co-existing secondary crack face that grows near the outer free plate surface. The dashed lines indicate crack edges visible to an observer on the outer free plate surface, while solid lines indicate the leading edge of the primary and secondary crack faces. In Fig. 7a, the shear lip is shown in perspective, while it is rotated in Fig. 7b so that the crack propagates toward the reader. The zero plane (x_1x_2-plane) that holds the leading crack tip lies above the current scanning region (in the positive x_3-

direction) and it is, thus, not part of Fig. 7. However, by comparing Fig. 6 to Fig. 7b it is obvious that by lowering the cross-sectional x_1x_2-plane from the zero-plane, in negative x_3-direction, the secondary crack face will first intersect the plane (and thereby appear first) at the outer free plate surface, but without connection to the primary slant crack face in that particular x_1x_2-plane (just as it was noticed from Figs. 4-6). By continuously lowering the plane of view, the secondary crack face grows and eventually connects to the primary slant crack face. It is also obvious from the three dimensional view in Fig. 7a that the curved crack visible on the outer free plate surface (dashed lines) is, in fact, the evolving shear lip (bear in mind that the history of the surface crack are easy to trace and indeed time resolved). Thus, the flipping mechanism truly initiates by the formation of small shear lips well behind the tunneling primary slant crack tip. Naturally, the shear lips propagate in an angle to the primary crack with the leading edges of the shear lip and the primary crack face intersecting at one point that defines the fracture surface morphology of the completed flip (studied in El-Naaman and Nielsen, 2013).

For a more complete overview of the crack tip flipping mechanism, Figs. 8-10 illustrate both automatically and manually generated reconstructions of the scanning data for intermediate resolution (20μm). Figure 8 display the crack tip in perspective, whereas Figs. 9 and 10 give a front and a top view, respectively. For the crack tip considered it is clear that the majority of the crack face (the primary crack) remains slanted in the x_2x_3-plane, whereas two shear lips (secondary crack faces) have formed near the outer free plate surface (see Fig. 8). The crack growth direction is along the x_1-axis, about which the flipping mechanism poses 180 degree rotational symmetry (also seen from cross-sectional views in Fig. 3). Moreover, it is clear from Fig. 8 that, at this state of the flip, the primary slant crack face propagates by moderate tunneling, with the tunnel extending approximately one plate thickness into the plate interior ahead of the visible crack on the outer free plate surface (see Fig. 10). This tunneling effect is to a wide extend governed by the severe thinning of the plate that takes place in front of the leading crack tip (see Figs. 5 and 8a). It is well known that with the localized thinning of the plate that takes place in the fracture process zone comes an elevated stress triaxiality level at mid-thickness of the plate, which, in turn, drives the void growth to coalescence process. This inherent behavior of the explored ductile steel may also be the reason for the fairly sharp, and well defined, leading crack tip.

Compared to the established plate tearing modes (cup-cup, cup-cone, and slanting), where the formation of micro-cracks and their linkage takes place at the leading edges of the crack, the

crack tip flipping mechanism set itself apart by being affected by an event (the formation of shear lips) well behind the leading tip. In fact, the established tearing modes eventually reach stationarity (no changes to the near-tip stress/strain field), whereby all parts of the leading edge maintain the same velocity. However, it is obvious from the present study that this cannot be the case during crack tip flipping. The crack tip stress and strain changes as the shear lips evolve and once a flip is completed – a new can begin.

What drives the "flipping" action is yet to be fully understood, but the out-of-plane deflection that develops due to loss of symmetry when slanting of the crack occurs, and any restriction on this deflection, is the prime suspects (see also Nielsen and Hutchinson, 2017). Once the failure process localizes into a shear band, and crack slanting occurs, an asymmetry in the near-tip stress/strain fields arise, and an out-of-plane deflection develops. This gives rise to combined mode I - mode III loading on the crack tip and thereby inducing an asymmetry in the fields (effective stress, stress triaxiality and Lode parameter) which govern the void nucleation/growth mechanism in ductile failure.

4. Concluding remarks

An experimental investigation of the crack tip flipping mechanism, observed for mode I slanted crack propagation in plate metals, has been conducted using X-ray tomography. The focus is on one particular crack tip where the flip is underway, and in that sense contrasts the initial study in El-Naaman and Nielsen (2013), were an already complete flip was investigated. Thus, the present study sheds light on the very initiation of the flipping and yields new insight into the changes of the leading crack front as the shift, from one 45-degree slant orientation to the opposite, takes place. The key findings of the study are:

- *Initiation of the flipping* is governed by the formation of shear-lips at the outer free plate surface, and all experimental results indicate that these secondary crack faces developed simultaneously such that the flipping poses 180-degree rotational symmetry about the growth direction (x_1-axis) - both on the final fracture surface and as the flip progresses. Thus, the initiation of the flip depend on an event that takes behind the leading tip, as the shear-lips form long before the leading crack tip show any sign of flipping.
- *During flipping* the crack tip consists of two types of leading edges; i) one being the leading edge of the primary slant crack face that holds the very crack tip, and ii) one being the leading edge of the evolving shear-lips. Initially, the leading edges of the shear-lips are small compared to the primary slant crack, but upon loading, the shear-lips will grow and

eventually take over to define the new orientation of the propagating crack. It is worth noticing that; since the shear-lips are responsible for forming a slanted crack to the opposite side, these necessarily have to travel at a greater speed than the leading edge of the primary crack. Relating the results in Fig. 10b to that of Fig. 5 in El-Naaman and Nielsen (2013) no evidence is found to supports that the leading edge of the primary crack face stops evolving when the shear-lips initiate.

- *The flipping process* contrasts slant crack propagation, where the crack remains oriented in one 45-degree shear-band and stationary stress/strain fields develop in the vicinity of the tip (no changes are seen by an observer traveling with the crack tip). Such stationarity cannot exist once the flipping action kicks-in as the near-tip fields naturally will change continuously as the shear-lips develop and the flip progresses. Moreover, once the crack has completed the flipping process, the subsequent slant crack propagation is typically limited to few (or even a fraction of) plate thicknesses before new shear-lips form and a new flip evolves.

The final stage of the flipping remains to be brought out. For example, details on the late stage of the crack front, when the shear-lips catch up with the leading slant crack tip, are unknown. However, from the present study it has become clear that the shear-lips eventually take over the leading slant crack and complete the flip. The crack tip, hereafter, continues to grow in this new orientation before shear-lips again initiate a flip to the opposite side. Creating an X-ray tomography *in situ* investigation while the entire flipping takes place seems a natural extension of the work presented, but despite the very stable nature of the flipping action, this poses significant challenges.

Acknowledgements

The work is financially supported by the VILLUM FOUNDATION Young Investigator Programme in the project "A New Phenomenon Yet to be Resolved in ductile PLATE tearing", grant VKR023451. The 3D Imaging Center at The Technical University of Denmark is gratefully acknowledged. Moreover, the authors acknowledge Dr. Pawel Woelke, Thronton Tomasetti Inc., and Dr. Ken Nahshon, Naval Surface Warfare Center Carderock Division, US Navy, for the many fruitful discussions of the work.

References

Barsoum, I., Faleskog, J., Rupture mechanisms in combined tension and shear - experiments, Int. J. Solids Struct. 2007a;44:5481-5498.

Barsoum, I., Faleskog, J., Rupture mechanisms in combined tension and shear - micromechanics, Int. J. Solids Struct. 2007b;44:5481-5498.

Benzerga, A., Micromechanics of coalescence in ductile fracture, Journal of the Mechanics and Physics of Solids, 2002;50:1331-1362.

Benzerga, A., Leblond, J.-B., Ductile Fracture by void growth to coalescence, Advances in Applied Mechanics, 2010;44:169-305.

Besson, J. Steglich, D., Brocks, W., Modelling of plane strain ductile rupture, Int. J. Plasticity, 2003;19:1517-1541.

El-Naaman, S.A., Nielsen, K.L., Observations on Mode I ductile tearing in sheet metals, European J. Mech. A/Solids, 2013;42:54-62.

Feldkamp, L.A, Davis, L.C., Kress, J.W, Practical cone beam algorithm, J. Opt. Soc. Am. A: Optics Image Sci. 1984;1:612-619.

Felter, C.L., Nielsen, K.L., Assisted crack tip flipping under mode I thin sheet tearing, European J. Mech. A/Solids, 2017;64:58-68.

Fleck, N.A., Hutchinson, J.W., Void growth in shear, Proc. R. Soc. (London), 1986;A407:435-458.

Gruben, G., Hopperstad, O.S., Børvik, T., Simulation of ductile crack propagation in dual-phase steel, Int. J. Frac., 2013;180:1-22.

Gurson, A., Continuum theory of ductile rupture by void nucleation and growth - I. Yield criteria and flow rules for porous ductile media, J. Eng. Mater. Technol., 1977;9:2-15.

Koplik J., Needleman, A., Void growth and coalescence in porous plastic solids, Int. J. Solids Struct. 1988;24:835-853.

Leblond, J.-B., Motlet, G., A theoretical approach of strain localization within thin planar bands in porous ductile materials, C.R. Mecanique, 2008;336:176-189.

Liu, B., Qiu, X., Huang, Y., Hwang, K.C., Li., M. Liu, C., The size effect on void growth in ductile materials, J. Mech. Phys. Solids, 2003;51:1171-1187.

Mathur, K., Needleman, A., Tvergaard, V., Three dimensional analysis of dynamic ductile crack growth in a thin plate, Journal of the Mechanics and Physics of Solids, 1996;44:439-464.

Morgeneyer, T.F., Taillandier-Thomas, T., Helfen, L., Baumbach, T., Sinclair, I., Roux, S., Hild, F., In situ 3-D observation of early strain localization during failure of thin Al alloy (2198) sheet, Acta Materialia, 2014;69:78-91.

Needleman, A., Void growth in an elastic-plastic medium, J. App. Mech., 1972;38:964-970.

Nielsen, K.L., Hutchinson, J.W., Steady-state, elastic-plastic growth of slanted cracks in symmetrically loaded plates, Int. J. Impact Eng. 2017 (in press), http://doi.org/10.1016/j.ijimpeng.2017.03.015.

Nielsen, K.L., Hutchinson, J.W., Cohesive traction-separation laws for tearing of ductile metal plates, Int. J. Impact Eng. 2012;48:15-23.

Nielsen, K.L., Tvergaard, V., Failure by void coalescence in metallic materials containing primary and secondary voids subject to intense shearing, Int. J. Solids Struct., 2011;48:1255-1267.

Pardoen, T., Hachez, F., Marchioni, B., Blyth, F., Atkins, A., Mode I fracture of sheet metal, Journal of the Mechanics and Physics of Solids, 2004;52:423-452.

Pineau, A., Benzerga, A.A., Pardoen, T., Failure of metals I: Brittle and ductile fracture, Acta Materialia, 2016;107:424-483.

Rivalin, F., Pineau, A., Di Fant, M., Besson, J., Ductile tearing of pipeline-steel wide plates - I. dynamic and quasi-static experiments, Eng. Frac. Mech., 2001;68:329-345.

Scheyvaerts, F., Onck, P.R., Bréchet, Y., Pardoent, T., Void growth and coalescence under general loading conditions, Report Université catholique de Louvain, 2006.

Simonsen, B.C., Törnqvist, R., Experimental and numerical modelling of ductile crack propagation in large-scale shell structures, Marine Structures, 2004;17:1-27.

Thomason, P.F., Ductile Fracture of Metals, Pergamon press, 1990.

Tvergaard, V., Influence of voids on shear band instabilities under plane strain conditions, Int. J. Frac., 1981;17:389-407.

Tvergaard, V., Ductile fracture by cavity nucleation between larger voids, J. Mech. Phys. Solids, 1982a;30:265-286.

Tvergaard, V., Influence of void nucleation on ductile shear fracture at a free surface, J. Mech. Phys. Solids, 1982b;30:399-425.

Tvergaard, V., Material failure by void growth to coalescence, Adv. Appl. Mech., 1990;27:83-151.

Tvergaard, V., Shear deformation of voids with contact modeled by internal pressure, Int. J. Mech. Sci., 2008;50:1459-1465.

Tvergaard, V., Behaviour of voids in a shear field, Int. J. Frac., 2009;158:41-49.

Zheng, L., Petry, D., Rapp, H., Wierzbicki, T., Mode I fracture of large-scale welded thin-walled AA6051 extruded panels, Thin-Walled Structures, 2009;47:375-381.

Tables

Table 1: Mechanical properties of the normal strength steel considered.

Parameters	**Notation**	**Value**	**Origin**
Young's modulus	E	210 [GPa]	Estimated
Poisson ratio	ν	0.3	Estimated
Yield stress (0.2% strain)	$\sigma_{0.2}$	256.7 [MPa]	From uni-axial tension data
Peak Stress	σ_{peak}	512.3 [MPa]	From uni-axial tension data
Yield stress	σ_y	160.6 [MPa]	From fitting;
Strain hardening	N	0.203	$\frac{\sigma}{\sigma_y} = \left(\varepsilon E/\sigma_y\right)^N$

Figures

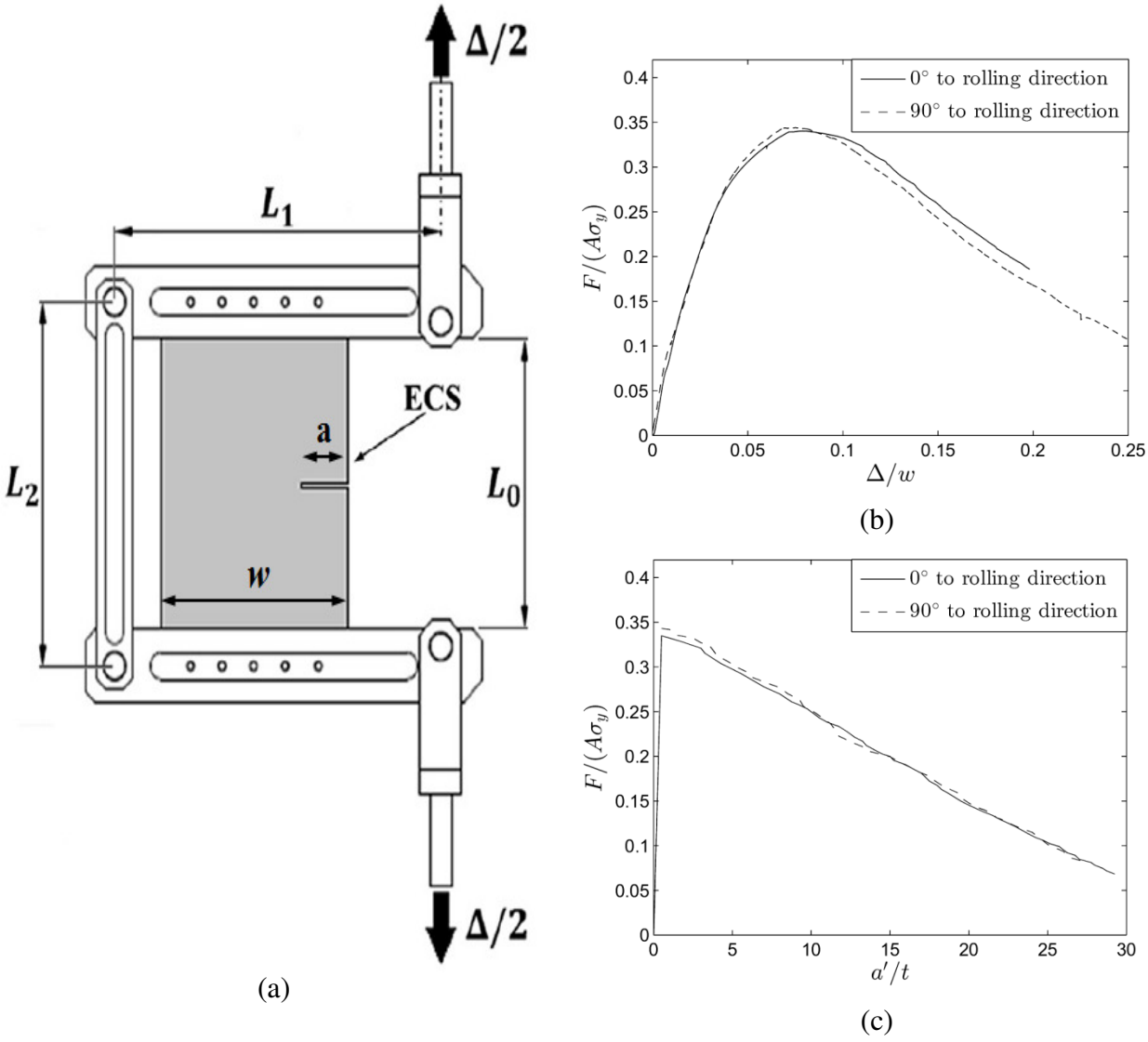

(a) (b) (c)

Figure 1: Experimental plate tearing test set-up. (a) Schematic of the mechanical grips and test specimen (single edge crack specimen, in gray), (b) measured force-displacement curve, and (c) measured force versus crack extension. All measurements are made for normal strength steel with the crack growing either normal or transverse to the rolling direction of the sheet (see also El-Naaman and Nielsen, 2013). The dimensions are; $L_0 = 250$mm, $L_1 = 350$mm, $L_2 = 313$, $w = 200$mm, and $a = 50$mm.

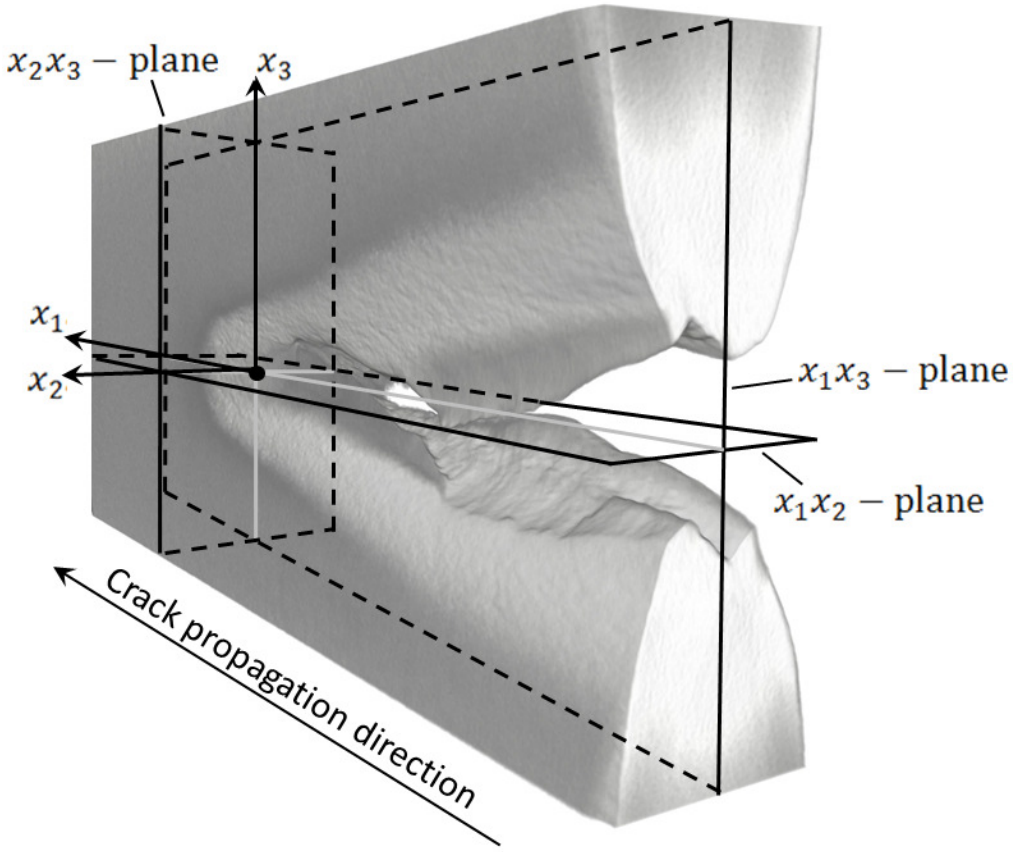

Figure 2: 3D perspective of the flipping crack with the global coordinate system defined by the three zero-planes. Origo is located at the leading crack tip (indicated by the black dot) and the positive x_1-axis is in the crack propagation direction.

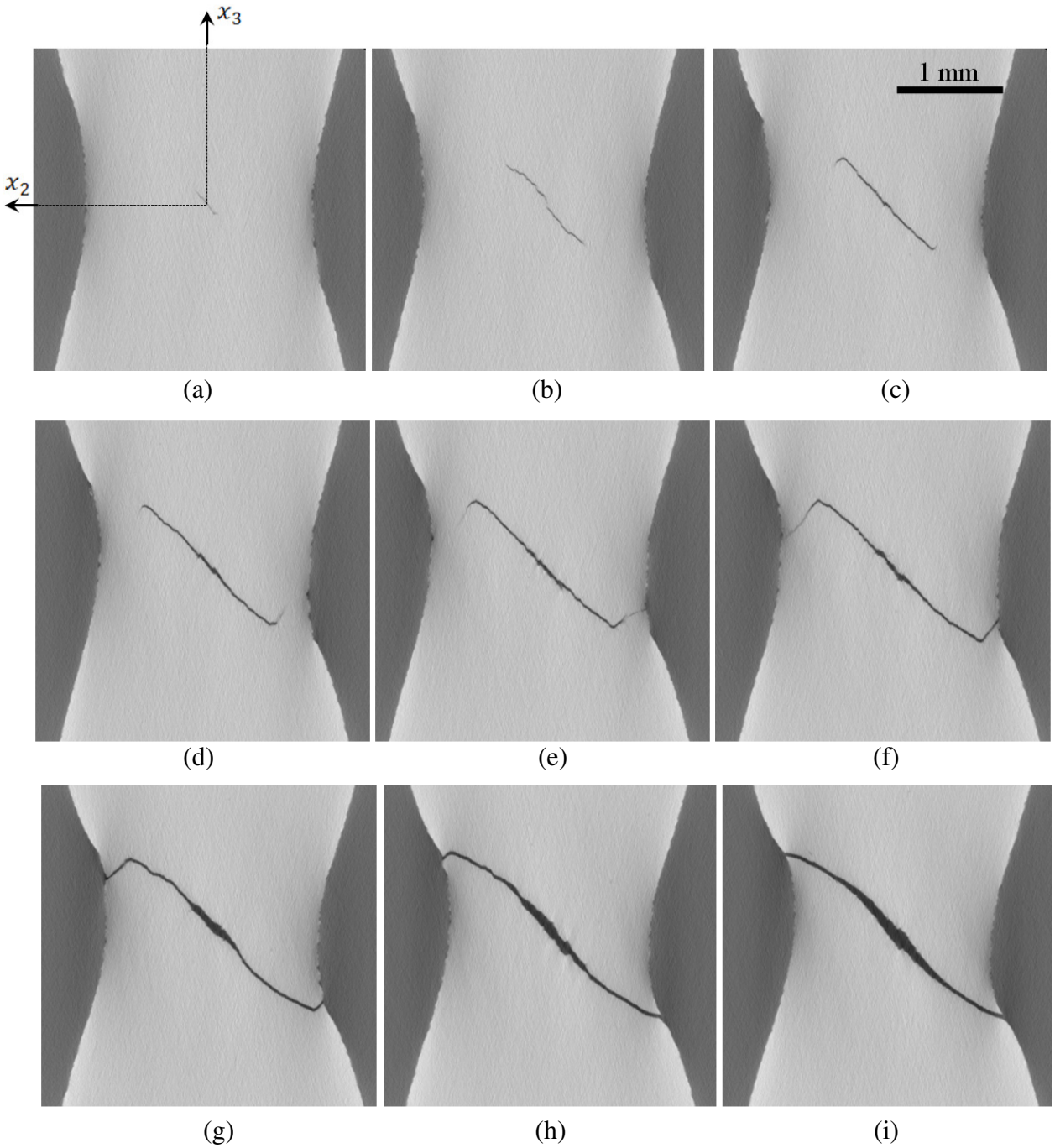

Figure 3: Cross-sectional view of the flipping crack (x_2x_3-plane) with the crack growing perpendicular to the cross-section and away from the reader. Here, near tip orientation of the slant crack in (a) and the evolution of this slant primary crack in (b) and (c), to the initiation of the flipping action in (d) and the evolution of the flip in (g) to (h). Far behind the crack tip a slant crack exists in (i). The X-ray tomography results are shown for a resolution of $\sim 20\mu$m, and the images corresponds to cross-sections located at (a) $\sim -80\mu$m, (b) $\sim -360\mu$m (c) $\sim -640\mu$m, (d) $\sim -800\mu$m, (e) $\sim -880\mu$m, (f) $\sim -960\mu$m, (g) $\sim -1160\mu$m, (h) $\sim -1360\mu$m, and (i) $\sim -1680\mu$m relative to the coordinate system defined by the zero-planes specified in Fig. 2.

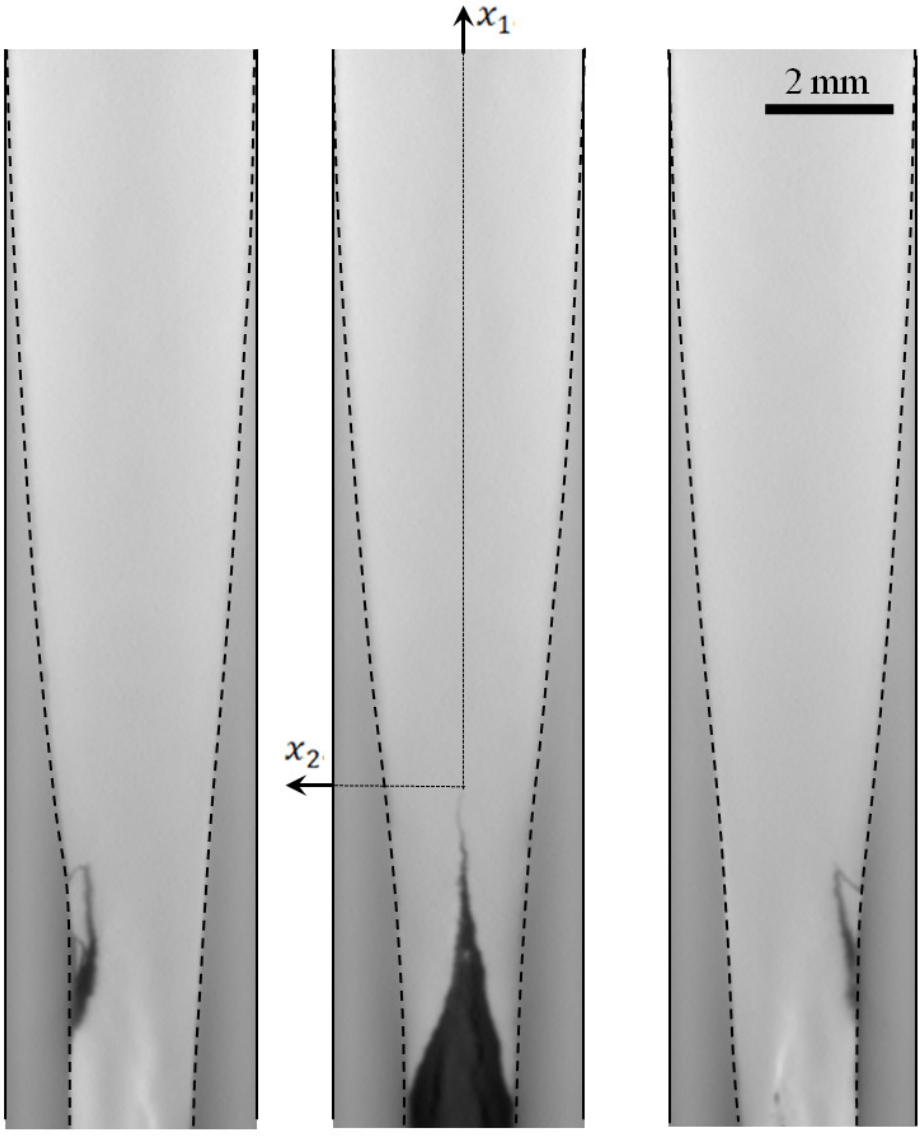

(a) (b) (c)

Figure 4: Cross-sectional overview of the crack propagation in the x_1x_2-plane with a resolution of the X-ray tomography scan of $\sim 100\mu$m. Here, showing the intense thinning region governing the crack growth. Cross-sections are located at (a) $\sim 469\mu$m, (b) zero x_1x_2-plane, and (c) $\sim -632\mu$m relative to the coordinate system defined by the zero-planes specified in Fig. 2.

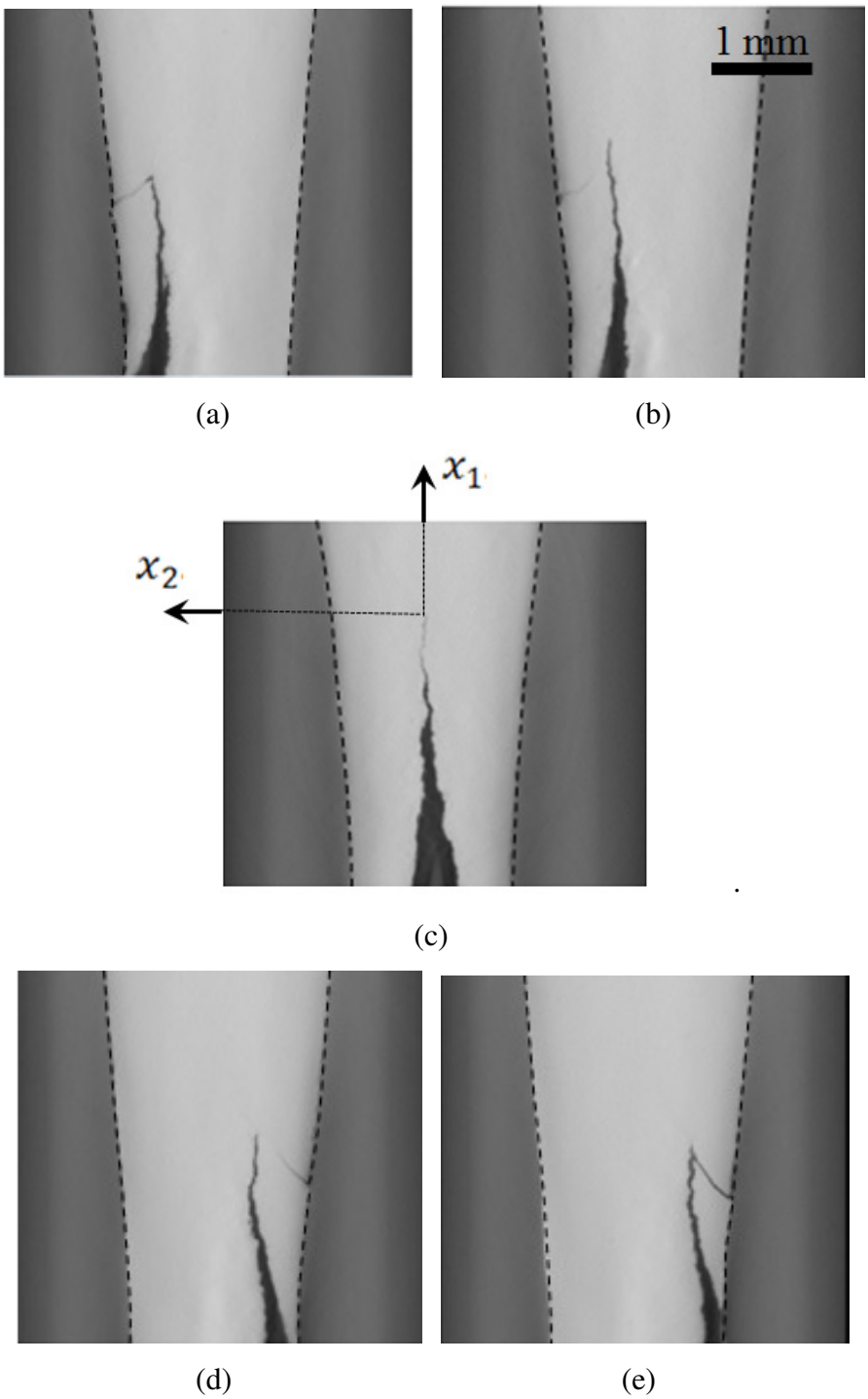

Figure 5: Cross-sectional view of the crack propagation in the x_1x_2-plane with a resolution of the X-ray tomography scan of $\sim 20\mu$m. Here, displaying the location and evolution of shear-lips. Cross-sections are located at (a) $\sim 428\mu$m, (b) $\sim 344\mu$m (c) zero x_1x_2-plane, (d) $\sim -376\mu$m, and (e) $\sim -488\mu$m relative to the coordinate system defined by the zero-planes specified in Fig. 2.

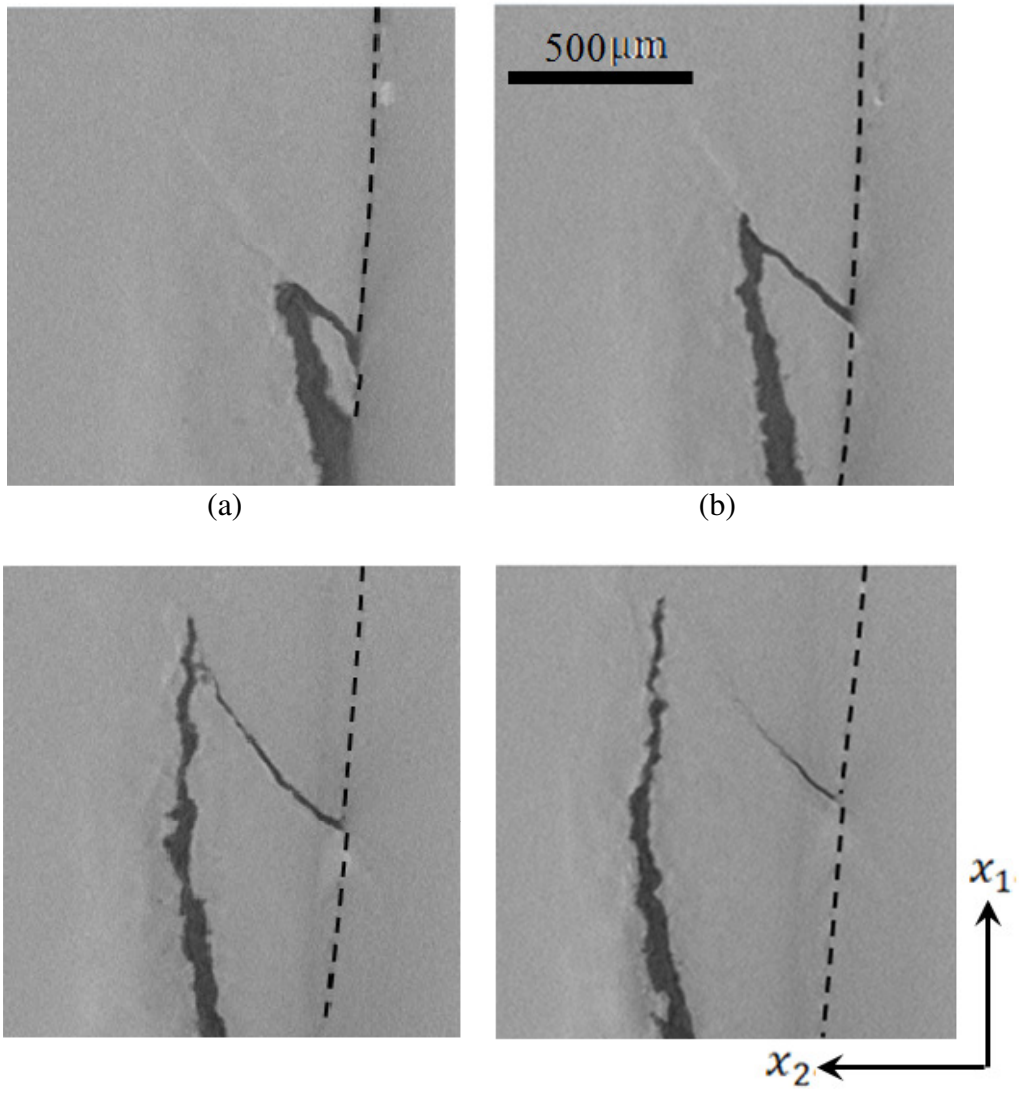

Figure 6: Cross-sectional view of the crack propagation in the x_1x_2-plane with a resolution of the X-ray tomography scan of $\sim 6\mu$m. Here, displaying details of the evolution of a shear-lip. Relative to the cross-section in (a), the remaining cross-sections are located at; (b) $\sim 48\mu$m (c) $\sim 152\mu$m, and (d) $\sim 212\mu$m.

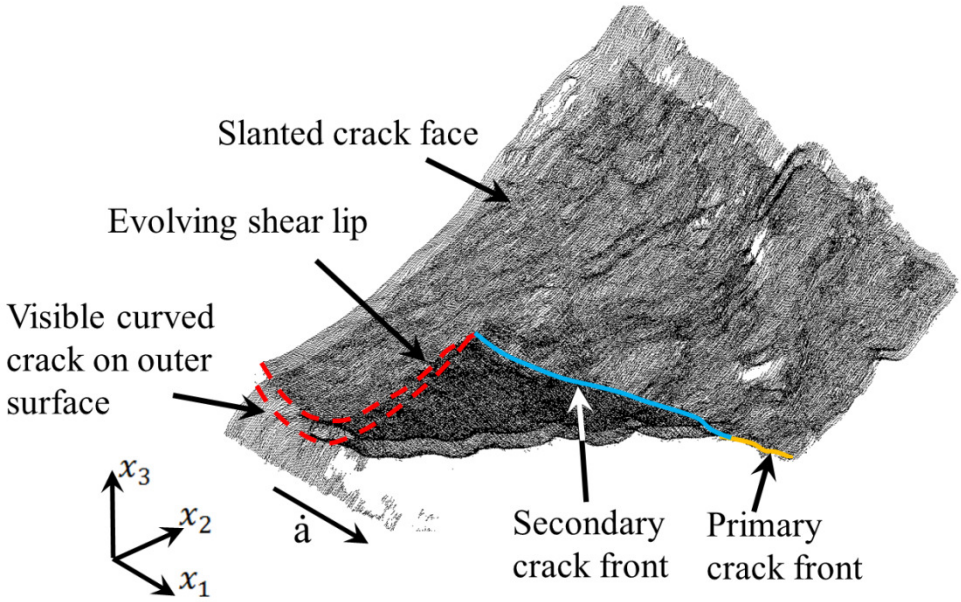

(a)

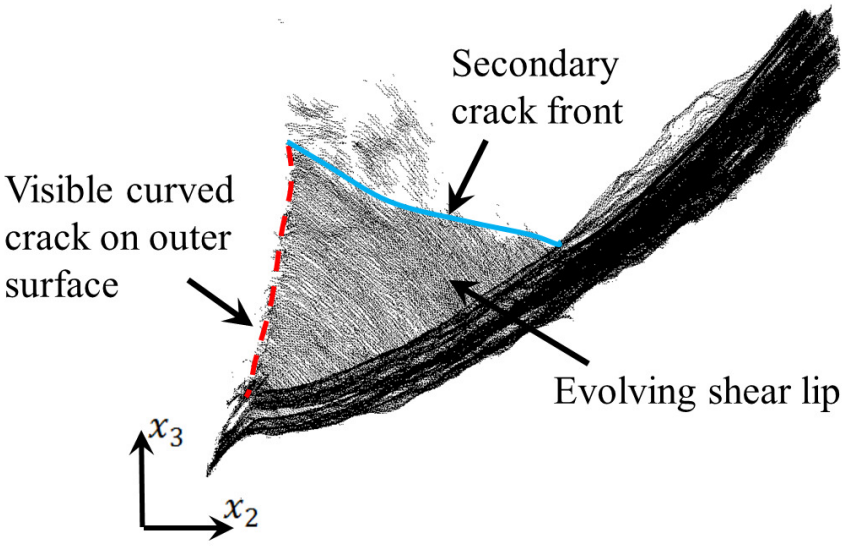

(b)

Figure 7: X-ray tomography results with a resolution of ~6μm, showing one shear-lip close to the outer free surface within the thinning region. The perspective in (a) correlates with that of Fig. 8 and the crack growth direction is indicated by $\dot{a}$ (to the right and towards the reader), whereas (b) correlates with Fig. 9, whereby the crack propagates toward the reader (the coordinate system defined by the zero-planes in Fig. 2 is maintained).

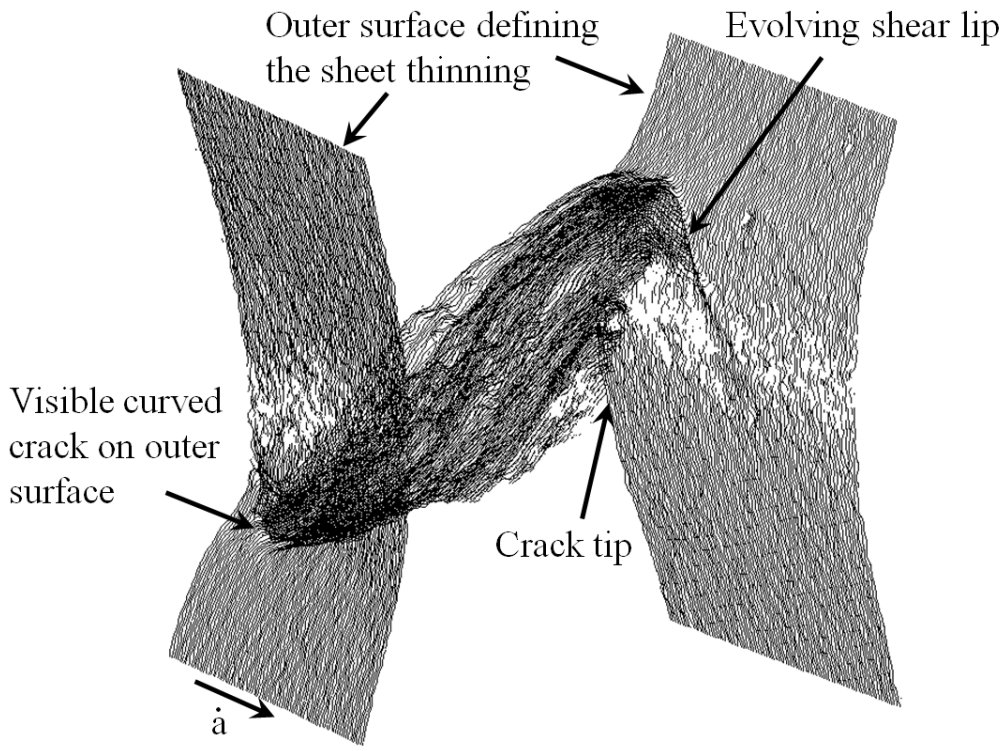

(a)

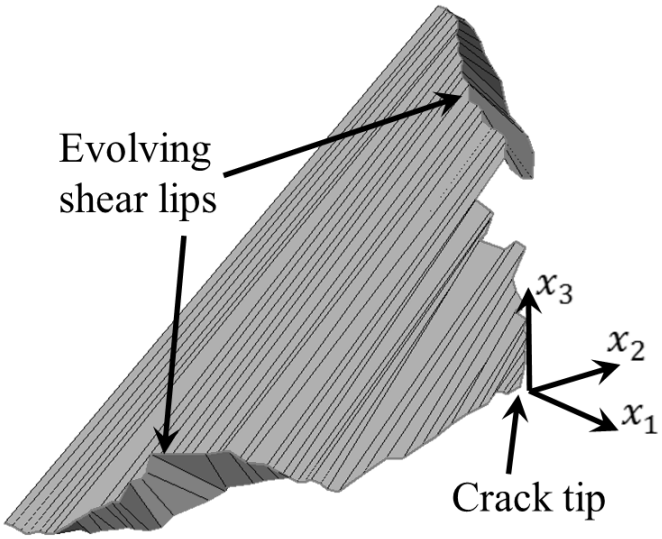

(b)

Figure 8: (a) X-ray tomography results with a resolution of ~20μm (intermediate), showing in perspective the flipping crack tip and outer surfaces that define the thinning region. The crack growth direction is indicated by $\dot{a}$ (to the right and towards the reader). (b) Reconstruction of the flipping crack tip based on manual analysis of the individual cross-sections.

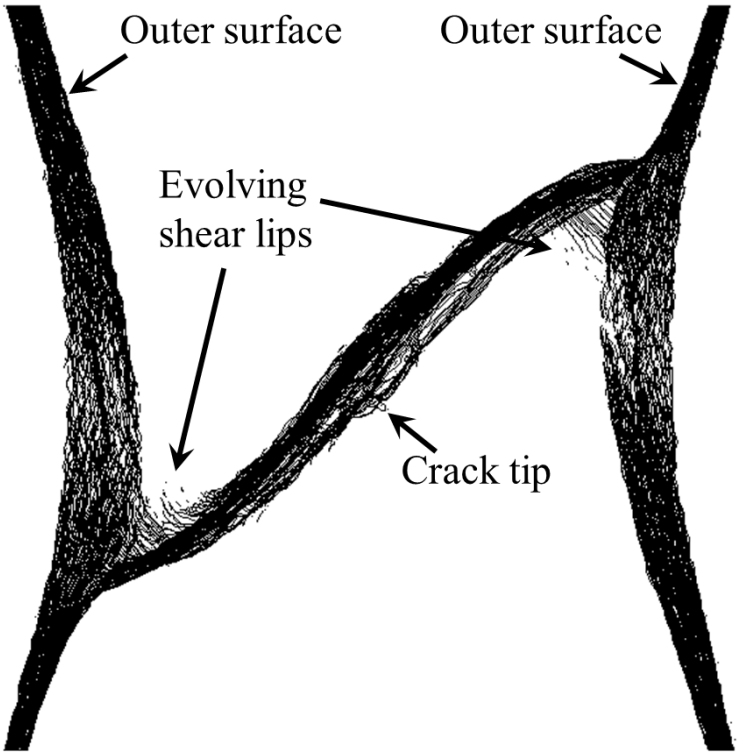

(a)

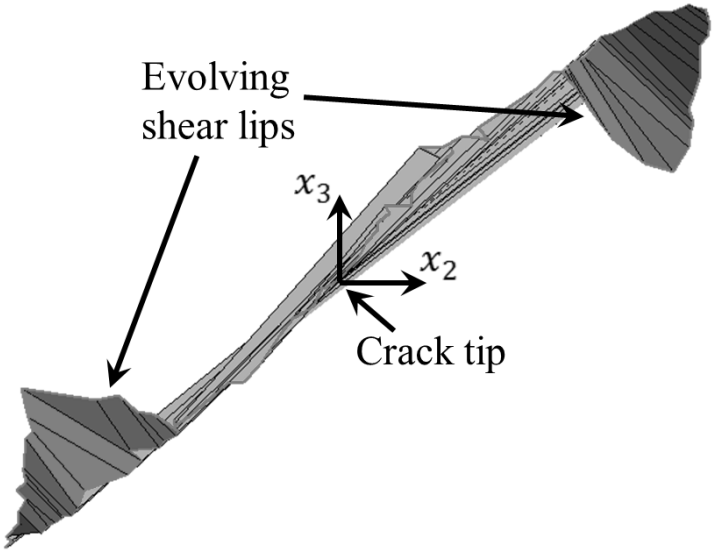

(b)

Figure 9: (a) Front view (x_2x_3-plane) of the X-ray tomography results with a resolution of ~20μm (intermediate), showing the flipping crack tip and outer surfaces that define the thinning region. The crack grows toward the reader. (b) Reconstruction of the flipping crack tip based on manual analysis of the individual cross-sections.

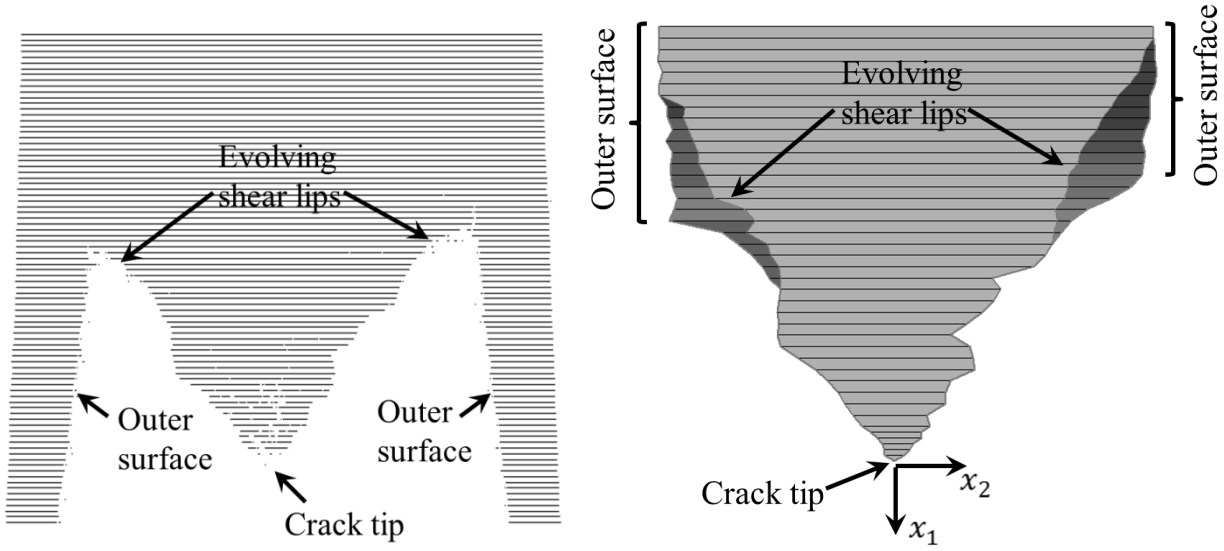

(a) (b)

Figure 10: (a) Top view (x_1x_2-plane) of the X-ray tomography results with a resolution of 20μm (intermediate), showing the flipping crack tip and outer surfaces that define the thinning region. (b) Reconstruction of the flipping crack tip based on manual analysis of the individual cross-sections.